



# Dynamic Time Division Scheduling Protocol for Medical Application Using Frog Synchronization Algorithm

Norhafizah Muhammad and Tiong Hoo Lim<sup>(✉)</sup>

Universiti Teknologi Brunei, Gadong, Brunei  
norhafizah.muhammad@utb.edu.bn, lim.tiong.hoo@utb.edu.bn

**Abstract.** Different wireless sensing methods have been proposed for acquisition and measurement of body signals. In medical healthcare, it is critical that data are received simultaneously, processed, and analyzed in order to diagnose the disease accurately. For instance, to detect a patient with sleep apnea, it is necessary for the biosignals from dozens of biosensors including electroencephalography (EEG), electrocardiogram (ECG), photoplethysmogram (PPG), and peripheral oxygen saturation ( $SpO_2$ ) to be received in sequence it is used for diagnosis. However, it is difficult to accurately received these signals as their measurement frequencies are different from each other. Precise synchronization of the heartbeat with other measuring cycles of each biosensor is a critical attribute for identifying the correlation of each biosignal. Carrier Sense Multiple Access with Collision Avoidance (CSMA/CA) used in existing body area networks to guarantee the precise synchronization of multi-biosignals. This paper addressed this issue by proposing a bio-inspired Dynamic Time Division Scheduling Protocol (D-TDSP) based on the Frog Calling Algorithm (FCA) to adjust the timing of data transmission and to guarantee the synchronization of the sensing and receiving of multi-biosignals. The accuracy of the proposed algorithm is compared with the CSMA/CA method using a TelosB and XM1000 sensor nodes.

**Keywords:** Frog Calling Algorithm · Bio-inspired · Biosensor · Synchronization · Transmission data · Health monitoring

## 1 Introduction

Medical devices in the wireless body sensor networks (WBSNs) can be broadly divided into wired and wireless. Wired medical devices have high precision, but they are inconvenient to wear, complicated, and difficult to use by individual patients. In contrast, wireless medical devices are usually worn by the patient in the form of wearable devices making it more popular to be used at home for medical physiological monitoring and diagnosis [1, 8]. These devices can be

added to the networks as new or additional biometric needs to be collected. WBSNs consist of a number of short-range wireless communication devices. The biosensor on each device periodically receives biometric signal data through the connected biosensors. The biosensor can be embedded within the communication devices, or implant or attached outside the human body [3]. Each device is placed near the human body to collect data such as electrocardiograms, heart rate, and acceleration.

Individual device periodically receives the biometric data from the biosensor and transmit the signal collected to a centralised server for processing. Each device can perform time synchronization using periodic biosignal generated from the individual nodes. To analyze different biosignals received from different biosensor for medical diagnosis, it is necessary to read those biosignals from one or several devices accurately and periodically in a synchronised manner [2]. As the biosensor devices are attached at different body parts, signals arriving from several devices may not be synchronized with the measured time. According to Pflugradt et al. [7], biosignal measurements can be partially obstructed by environmental influences and motion artifacts as the patients are usually not at rest. Data acquisition devices like ECG and PPG sensors are can be disrupted due to contacts failure or shifting photosensor positions [7]. The presence of intermittent radio interference from other medical devices can also disrupt the bio-signal transmission of the nodes [6]. Hence, there is a need to develop a fault tolerance data transmission scheduling algorithm that can guarantee sensing data synchronization and sequencing to make accuracy medical diagnosis.

In this paper, a time division based scheduling algorithm is proposed that can adapt and adjust its firing time according to the environment without affecting the sensing data sequence and the synchronized transmission. The main contribution of this paper is the development and analysis of a novel Bio-inspired algorithm called Dynamic Time Division Scheduling Protocol (D-TDSP) for Wireless Biosensor Networks (WBN) that capture and transmit the biomedical signals according to actual diagnosis pathway for a disease. The D-TDSP dynamically allocated the transmission time for each node using a modified Time Division Multiple Access (TDMA) approaches based on Frog Calling Algorithms (FCA).

The analysis from hardware experimental results have shown that the proposed D-TDSP is tolerate to single point of failure as there is no centralised control on the transmission scheduling. Individual node can adjust its transmission period according to the transmission time of its neighboring nodes. The proposed algorithm can also adapt to network changes due to device addition, and node removal or temporary anomaly due to interference compare to Firefly Synchronization (FAST) or default CSMA/CA.

Section 2 presents the basic background on the works related to time synchronization and scheduling in WBSNs followed by the design of the proposed algorithm in Sect. 3. In Sect. 4, the scenario and experimental setup used for the evaluation of the proposed D-TDSP are described. Section 5 and 6 discusses

and validates the results obtained from the hardware experiments using a combination of two types of nodes. In Sect. 7, we conclude with future research.

## 2 Remote Healthcare Diagnosis and Detection

The WBSN can be used to sense, monitor, capture and extract physiological information of a patient using biosensor such as the electroencephalography (EEG), electrocardiogram (ECG), photoplethysmogram (PPG), and peripheral oxygen saturation ( $SpO_2$ ) [5]. They can also be used to assist in other aspects of a patient's care, such as reporting on the current real-time location of a patient, recording a patient's condition for later analysis, or communicating a patient's condition to a remote party, such as a hospital or physician. These biosensor node can be attached or implanted to the patient's body [10].

WBSN applications need to be easy to use and with minimal user configuration. The attached biosensors should not intervene with the patient daily activities. It should be able to deliver and manage the information related to the patient care remotely [8]. Each biosensor will have its own timing circuit with a local clock. The biosensor needs to be connected to the network and the communication timing between biosensor nodes need to be synchronized to transmit the biodata without interfering with another nodes.

Most of these functions require tight time synchronization to function properly especially for applications that require two or more parameters for diagnostic or treatment [9]. They usually involves time synchronization of multiple biosensors forming a dynamically network. These networks need to be reconfigurable automatically to allow the nodes to join or leave the network, or to overcome communication failure triggered by interference from other radio devices. Upon joining the network, each node in the WBSNs must synchronize with one another. This synchronization may account for a number of possible sources of time discrepancy, such as differences in time stamping, communications latency during signal transmittance and/or other sources.

### 2.1 Packet Synchronization in Medical Application

Time synchronization is critical for time-sensitive applications such as medical health [12] for diagnostic in an Artificial Intelligence based medical application [7]. Zong et al. [11] mentioned the applications of time synchronization can be collaborated, coordinated and localized the position of the nodes. They found out that these nodes require precise timing in order to cooperate and monitor the physical or environmental variables.

Fixed time synchronization algorithm has been used in the MAC layer to ensure that data can be collected and transmitted reliable at a predetermined interval. In fixed time synchronization, the transmission interval allocated to individual node is equally divided among a set of nodes within a time period. Each node will need to transmit at the assigned interval to avoid packet collisions using time division approaches. However, fixed time synchronization approach

is not suitable for medical application as the sensing data needs to be transmitted at any time when a critical event is detected. The default CSMA/CA transmission protocol at the MAC layer is prone to collision when the number of biosensor nodes increases. Hence, there is a need to apply bio-inspired synchronization algorithm at the application layer to ensure that the patient physiological data can be received promptly and reliably.

## 2.2 Frog Calling Synchronization Algorithm

The bio-inspired, Frog Calling Algorithm (FCA) is a self-organized control algorithm. This synchronization is based on the calling behavior of the Japanese Frog developed and modeled by Aihara et al. [4]. The main purpose of this frog behavior is to attract the female frog. The process is when there is a group of male frogs in the area, when one start calling, the others will start calling too. With the multiple calling, the female frog will have difficulties to distinguish which male frog is calling. Hence, they shifted the time of their calling [4]. Aihara et al. [4] developed a self-organizing scheduling scheme inspired by FCA for collision-free transmission scheduling in Wireless Sensor Networks. The authors evaluated their proposed algorithm in simulation and the results have shown that it can reduce the data transmission failures and improves the data collection ratio up to 24% compared to a random transmission method.

## 3 Dynamic Time Division Scheduling Protocol

In this section presents the algorithm framework of the D-TDSP. The D-TDSP allows the nodes fired evenly distributed within a time period. In a network, there are a set of number of nodes which work in a single hop topology. Each of the node will have the same period of time, where in this case  $T = 32$  kHz. Figure 1 below shows the process of the dynamic time division scheduling protocol approach.

Figure 1(a) shows the initial stage before the algorithm starts. All of the nodes seen are not in periodic and synchronized position. When node A fired, it will look for the previous node, which is node B and it will use the Eq. 1 to evaluate the new position. As soon as Node B jump to new position, B as shown in Fig. 1 (b) and consequently. This will be repeated with the other nodes. Each node will adjust its transmission position until all of the nodes are evenly spread within the length period of time of the basestation (as shown in Fig. 1(c) below).

$$f(x) = f^{-1}(f(t') - \epsilon) \quad (1)$$

The value of  $\epsilon$  is determined by Eq. 2, the mathematical equation shown below.

$$\epsilon = \left(\frac{t'' + t'}{2}\right)\alpha \quad (2)$$

where  $\alpha$  is a synchronization damping function.

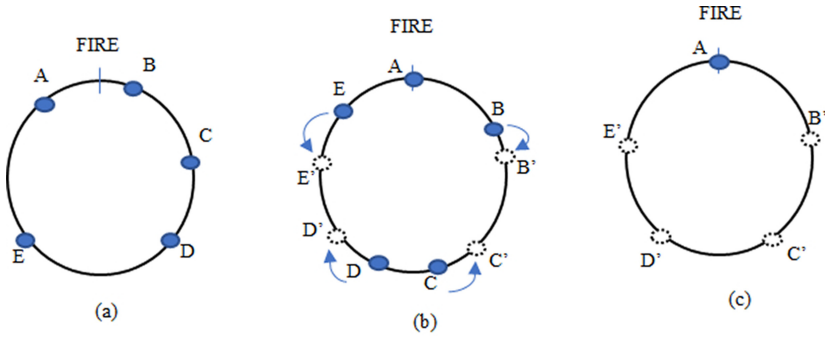


**Fig. 1.** Adaptive transmission scheduling algorithm (a) Node fires at a time period T. (b) Node responds to neighbors firing to adjust its firing timing between A and C

### 4 Experimental Setup

To evaluate the performance of D-TDSP against CSMA/CA random transmission and a firefly-inspired scheduling algorithm called Firefly Adaptive Scheduling Transmission (FAST), an xm1000 motes will be used as the WBN node. These nodes will be deployed in a similar manner to the application in the healthcare monitoring systems shown in Fig. 2. The bio sensors are to be attached on or implanted into the human body to collect physiological information such the electrocardiogram (ECG), electroencephalography (EEG), pulse rate, blood pressure, body temperature and (SpO<sub>2</sub>) and each biosensor will be connected to the XM1000 nodes. The WBSN will be operating in a star topology configuration, where all the data from the biosensor will be sent to the base station using single hop communications.

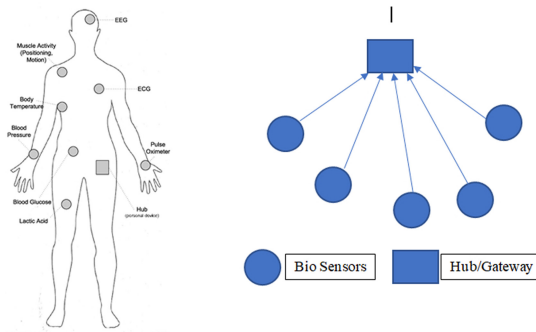


**Fig. 2.** The WBNs with biosensor attached to the body and a node to transmit the sensed data to the gateway.

A TelosB node will be used as a monitoring base station to collect the synchronization statistics and monitor the scheduling of the data transmission. XM1000 mote will be used as the individual sensor nodes that will collect the biodata to be transmitted within a clock cycle as shown in Fig. 3. Each nodes will have a unique id and the base station will need to capture the sequence and order of the packet received, and calculate the Packet Delivery Rate (PDR) using Eq. 3 below.

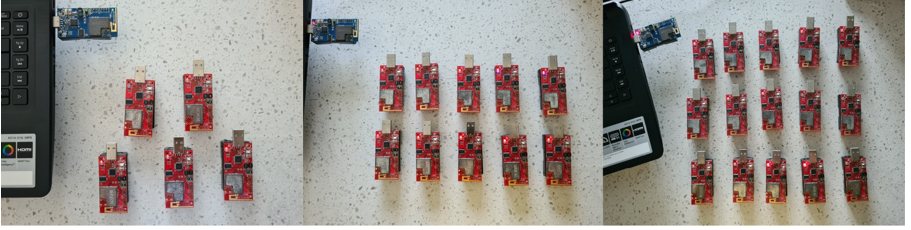


**Fig. 3.** The 5, 10, and 15 XM1000 nodes used for the experiment with one telosB mote connected to the notebook for data collection.

$$\text{Packet Delivery Ratio, } PDR = \frac{P_{rx} \times 100}{\sum_{i=1}^n P_G(i)} \quad (3)$$

Where  $P_{rx}$  is the total number of data packets received by the sink node and  $P_G$  is the packet generated by the source node.

Different numbers of 5, 10, 15 XM1000 motes were used to evaluate the scalability of the proposed algorithms as shown in Fig. 3. A laptop will be connected to the monitoring node to store and display the statistics collected. The synchronization process will begin when the first node starts to fire. The rest of the sensor nodes receiving the message will adjust its transmission period and transmit its own messages. This process will continue until the experiment ends.

Three set of experiments are conducted and repeated to compare the order of packet arrival at the base station and reliability in term of the PDR.

## 5 Results

In this section, the performance analysis of D-TDSP is compare against the random CSMA/CA and FAST. Three set of experiments are performed. The first experiment evaluates the sequencing of the packet received and the PDR against the network size for the three algorithms. The second and third experiments analyze the reliability of all the three algorithms when 1. a new node is added to the network and 2. When a node temporary fail to model scenario such as radio interference or node maintenance to replace battery.

### 5.1 Sequencing of Packet Delivered for 5 Nodes

In Fig. 4, Fig. 5 and Fig. 6 below show the synchronization process of the three synchronizations, the D-TDSP, FAST and CSMA/CA. It can be seen that the D-TDSP and FAST synchronization can achieved synchronization within the period of time as shown in Fig. 4 and Fig. 5 respectively. By observing the FAST synchronization process in Period 3, when all of the nodes transmitted it shows that the nodes were then in sleep mode for a short time before going into Period 4. In the D-TDSP, the nodes in Period 4 can be seen that it broadcasted the data in an evenly manners. While in CSMA/CA shown in Fig. 5 shows that the nodes transmit at a synchronicity patterns but the firing time will be at random and the nodes will only fire from the previous cycles.

However, when analysing the data arriving sequence of D-TDSP transmission shows that all the nodes have broadcasted the data in a synchronous pattern for every 20 cycle, while in the FAST and CSMA/CA only managed to synchronised 10% and 30% of every 20 cycles respectively. The FAST has the lowest synchronicity as the nodes will continuous to update the firing time even when synchronization is achieved.

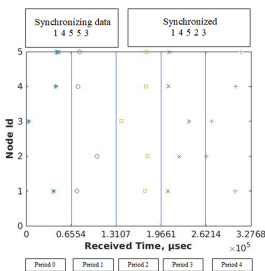


**Fig. 4.** The order of packet received by the basestation from 5 nodes for D-TDSP

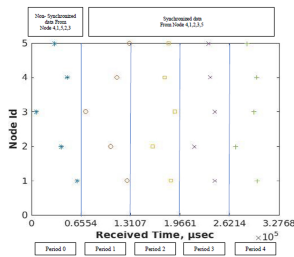


**Fig. 5.** The order of packet received by the basestation from 5 nodes for FAST

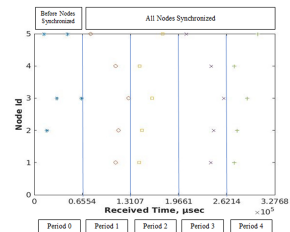


**Fig. 6.** The order of packet received by the basestation from 5 nodes for random CSMA/CA

### 5.2 Statistical Test on the Synchronization Period for 5 Nodes

In the average synchronization period shown in Table 1, the D-TDSP and the CSMA/CA approach have consistent average period through out the process compare to FAST. This means that the transmission period for the nodes are equally distributed and each node always transmit at the allocated time within the period. The p-value obtained in the T-Test also shown that the transmission period is statistically significant. Hence, the results show that the D-TDSP performs better compared to the FAST synchronization and CSMA/CA and can broadcast in a synchronized and evenly distributed patterns when the numbers of nodes is small.

**Table 1.** Average of synchronization period for 5 nodes.

Node ID	D-TDSP		FAST		Random CSMA/CA	
	Av. cycle period	p-value	Av. cycle period	p-value	Av. cycle period	p-value
1	35800.00	$7.10 \times 10^{-68}$	56192.03	$1.11 \times 10^{-36}$	32254.90	$1.14 \times 10^{-9}$
2	35800.00	$6.22 \times 10^{-58}$	50840.00	$3.72 \times 10^{-24}$	32254.90	$1.14 \times 10^{-9}$
3	35800.00	$6.22 \times 10^{-58}$	49125.47	$9.13 \times 10^{-22}$	32254.90	$1.14 \times 10^{-9}$
4	35800.00	$6.22 \times 10^{-58}$	49841.18	$1.27 \times 10^{-22}$	32254.90	$1.14 \times 10^{-9}$
5	35800.00	$6.22 \times 10^{-58}$	49771.47	$2.87 \times 10^{-23}$	32254.90	$1.14 \times 10^{-9}$

### 5.3 Sequencing of Packet Delivered for 10 Nodes

The packet arrival sequences for 10 nodes transmitting in the networks is shown in Fig. 7, Fig. 8 and Fig. 9.

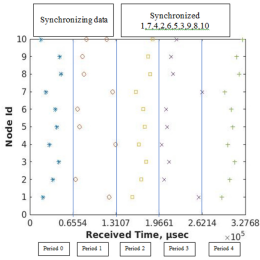


**Fig. 7.** The order of packet received by the basestation from 10 nodes for D-TDSP

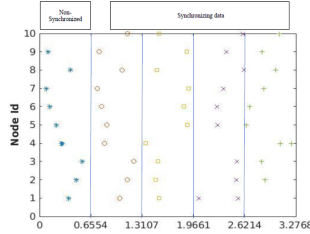


**Fig. 8.** The order of packet received by the basestation from 10 nodes for FAST

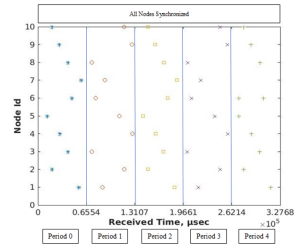


**Fig. 9.** The order of packet received by the basestation from 10 nodes random CSMA/CA

The results show that the D-TDSP allows each node transmitted in a synchronized and evenly distributed as the packets received are always in ordered. As for FAST, packets transmitted by all the nodes are received at the basestation but not in evenly distributed manners. This is because the nodes in the network were trying to align their time in order to collect the data simultaneously. The D-TDSP has achieved 100% synchronicity for every cycles throughout the transmission while FAST only achieves 10% synchronicity and CSMA/CA 70%. This means that data arrival schedule transmitted by the nodes in the network is not always the same for FAST.

### 5.4 Statistical Test on the Synchronization Period for 10 Nodes

In the statistical test shown in Table 2, the synchronization period shows that D-TDSP and the CSMA/CA have a consistent average cycle period at 34700.00  $\mu$ s



and 32063.34  $\mu\text{s}$  respectively as the p-value is  $\leq$  than 0.01. The consistent average period indicates the nodes in the networks always transmit at the allocated synchronized time. FOR CSMA/CA, the transmission time is configured in the program while for D-TDSP, each node will determine its own transmission based on its neighboring firing.

**Table 2.** Average of synchronization period 10 nodes.

Node ID	D-TDSP		FAST		Random CSMA/CA	
	Av. cycle period	p-value	Av. cycle period	p-value	Av. cycle period	p-value
1	34700.00	$3.35 \times 10^{-226}$	27387.62	$8.96 \times 10^{-22}$	32063.34	$9.35 \times 10^{-11}$
2	33800.00	$1.15 \times 10^{-209}$	34278.92	$1.12 \times 10^{-22}$	32063.34	$9.35 \times 10^{-11}$
3	34700.00	$1.12 \times 10^{-221}$	34278.92	$1.12 \times 10^{-22}$	32063.34	$9.35 \times 10^{-11}$
4	34700.00	$3.92 \times 10^{-227}$	34278.92	$1.12 \times 10^{-22}$	32063.34	$9.35 \times 10^{-11}$
5	34700.00	$4.00 \times 10^{-234}$	33344.77	$8.89 \times 10^{-22}$	32063.34	$9.35 \times 10^{-11}$
6	34700.00	$3.95 \times 10^{-289}$	34095.28	$7.82 \times 10^{-22}$	32063.34	$9.35 \times 10^{-11}$
7	34700.00	$3.08 \times 10^{-221}$	34233.08	$6.80 \times 10^{-18}$	32063.34	$9.35 \times 10^{-11}$
8	34700.00	$4.46 \times 10^{-209}$	33997.90	$4.63 \times 10^{-24}$	32063.34	$9.35 \times 10^{-11}$
9	34400.00	$9.45 \times 10^{-226}$	33366.90	$1.55 \times 10^{-21}$	32063.34	$9.35 \times 10^{-11}$
10	34100.00	$9.37 \times 10^{-230}$	34069.78	$2.39 \times 10^{-19}$	32063.34	$9.35 \times 10^{-11}$

## 5.5 Sequencing of Packet Delivered for 15 Nodes

In Fig. 10, Fig. 11 and Fig. 12 below show the synchronization process of the three synchronizations, the D-TDSP, FAST and CSMA/CA.

As the network size is increased to 15 nodes, D-TDSP has managed to broadcast the data to the basestation in an evenly distributed period of time. The D-TDSP had achieved 65% synchronicity. As for the FAST and CSMA/CA, they only managed to maintain 15% and 45% synchronicity respectively. This is due to the increase of interference between nodes during transmission. It is shown that the D-TDSP can avoid interference once the network has been synchronised.

## 5.6 Statistical Test on the Synchronization Period for 15 Nodes

When the number of nodes increases to 15, the average transmission period for each node is not consistent for every cycle in D-TDSP as shown in Table 3. This was because of the large scale of the nodes which can cause delay in transmission from the nodes, the signal period propagated between 32000.00  $\mu\text{s}$  and 34700.00  $\mu\text{s}$ . However, the difference in transmission cycle between the nodes is small compared to FAST which is between 32409.70  $\mu\text{s}$  and 35682.48  $\mu\text{s}$ . The p-value of  $\leq 0.01$  also shows that the transmission period for every cycles is statistically significant. This means that the nodes always transmit at the allocated time.

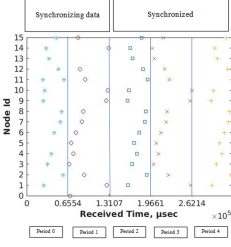


**Fig. 10.** The order of packet received by the basestation from 15 nodes using D-TDSP

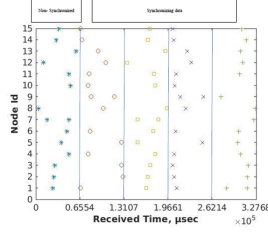


**Fig. 11.** The order of packet received by the basestation from 15 nodes using FAST

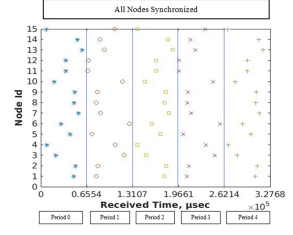


**Fig. 12.** The order of packet received by the basestation from 15 nodes using random CSMA/CA

**Table 3.** Average of synchronization period for 15 nodes.

Node ID	D-TDSP		FAST		Random CSMA/CA	
	Av. cycle period	p-value	Av. cycle period	p-value	Av. cycle period	p-value
1	33900.00	$6.16 \times 10^{-214}$	33722.83	$1.10 \times 10^{-74}$	32212.30	$1.09 \times 10^{-5}$
2	33900.00	$9.05 \times 10^{-203}$	35095.05	$8.44 \times 10^{-82}$	32745.67	$7.40 \times 10^{-5}$
3	34200.00	$1.52 \times 10^{-205}$	35095.05	$8.44 \times 10^{-82}$	31998.87	$4.15 \times 10^{-10}$
4	33800.00	$3.23 \times 10^{-197}$	35095.05	$8.44 \times 10^{-82}$	32105.40	$1.10 \times 10^{-5}$
5	34700.00	$4.00 \times 10^{-234}$	32273.12	$4.57 \times 10^{-86}$	31998.30	$1.15 \times 10^{-9}$
6	32000.00	$9.35 \times 10^{-178}$	35173.33	$1.38 \times 10^{-78}$	31999.47	$5.16 \times 10^{-10}$
7	34200.00	$1.04 \times 10^{-200}$	32409.70	$1.44 \times 10^{-76}$	31998.30	$1.01 \times 10^{-9}$
8	34200.00	$2.64 \times 10^{-281}$	33988.58	$7.14 \times 10^{-85}$	31999.50	$1.54 \times 10^{-5}$
9	34200.00	$8.78 \times 10^{303}$	35682.48	$4.59 \times 10^{-83}$	31999.40	$7.12 \times 10^{-10}$
10	33300.00	$1.87 \times 10^{-208}$	35009.18	$1.96 \times 10^{-78}$	32105.63	$1.10 \times 10^{-5}$
11	34200.00	$2.50 \times 10^{-207}$	34350.10	$2.76 \times 10^{-84}$	32105.40	$1.12 \times 10^{-5}$
12	33600.00	$2.44 \times 10^{-201}$	34383.87	$1.88 \times 10^{-82}$	32532.77	$4.30 \times 10^{-5}$
13	34200.00	$8.22 \times 10^{-285}$	34248.22	$3.32 \times 10^{-78}$	31998.63	$1.53 \times 10^{-9}$
14	34200.00	$3.18 \times 10^{-290}$	34248.22	$3.32 \times 10^{-78}$	31999.23	$2.08 \times 10^{-9}$
15	33300.00	$7.87 \times 10^{-194}$	34248.22	$3.32 \times 10^{-78}$	31999.17	$1.50 \times 10^{-9}$

## 5.7 Evaluation of Packet Delivery Rate

In term of the PDR, Fig. 13, Fig. 14 and Fig. 15 shows that the D-TDSP had a PDR of between 98.4% and 100%, while random CSMA/CA had a PDR of between 97% and 100%. For all the networks sizes, D-TDSP has managed to maintain the PDR of above 98% and is higher than the FAST and random CSMA/CA (Table 4).

## 5.8 The Scheduling Effect During Network Interference

In the next two section, two different type of interference are introduced to the networks to evaluate the ability of the three algorithms to maintain the synchronicity of the nodes in the WBN. In this section, a node will be temporary

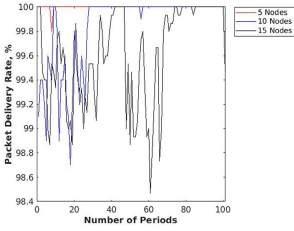


**Fig. 13.** The PDR using D-TDSP

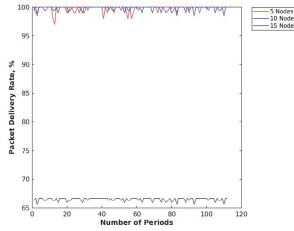


**Fig. 14.** The PDR using FAST

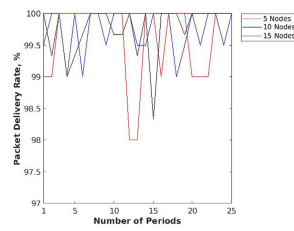


**Fig. 15.** The PDR using random CSMA/CA

**Table 4.** Average of Packet Delivery Rate (PDR) for 100 cycles for 5, 10, and 15 nodes.

No. of nodes	D-TDSP		FAST		Random CSMA/CA	
	Average PDR(%)	p-value	Average PDR(%)	p-value	Average PDR(%)	p-value
5	100	$1.84 \times 10^{-101}$	99.71	$1.62 \times 10^{-222}$	99.60	$1.56 \times 10^{-11}$
10	99.8	$1.36 \times 10^{-244}$	99.75	$1.03 \times 10^{-274}$	99.74	$2.81 \times 10^{-11}$
15	99.6	$7.53 \times 10^{-241}$	66.50	$3.93 \times 10^{-267}$	99.79	$1.65 \times 10^{-17}$

remove from the network to replicate the node battery replacement. Both experiments will measure and compare the packet arrival sequence in the base station for 5 and 10 nodes.

Figure 16, Fig. 17 and Fig. 18 show the synchronization periods of the D-TDSP, FAST and random CSMA/CA respectively for 5 nodes. It was observed that during the initial time, all of the three techniques shown that all of the nodes were in a synchronized pattern and in-phase. But when a node was added, the sensor nodes in D-TDSP can still maintain its synchronized pattern. While in CSMA/CA, the new nodes managed to transmit during the free slot. However, for FAST, the nodes are not in synchronicity. From the observation, FAST has difficulty in synchronizing the patterns, as the new node will interfere with the other nodes.

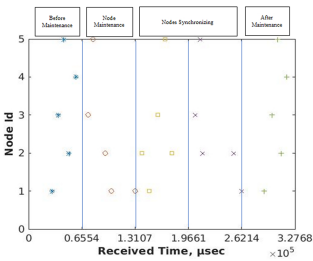


**Fig. 16.** Scheduling process of D-TDSP for 5 nodes when a node is removed temporarily

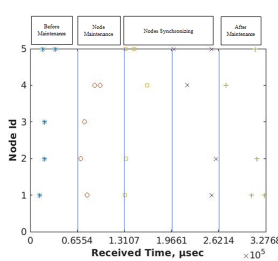


**Fig. 17.** Scheduling process of FAST for 5 nodes when a node is removed temporarily

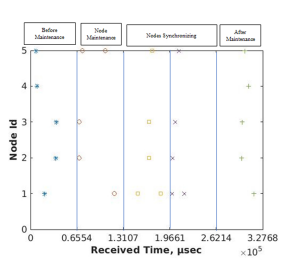


**Fig. 18.** Scheduling process of CSMA/CA for 5 nodes when a node is removed temporarily

In Fig. 19, Fig. 20 and Fig. 21, the scheduling effect for 10 nodes are presented. It can be seen that in FAST and D-TDSP, the nodes were able to transmit the data in synchronized patterns. By analysing the synchronicity nodes in every cycles, it is found out that D-TDSP has achieved 100% compared to the CSMA/CA and FAST (50% and 0% respectively). FAST has not been able to maintain the order of the packet received when a failure occurs.

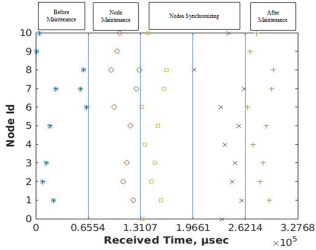


**Fig. 19.** Scheduling process of D-TDSP for 10 nodes when a node is removed temporary

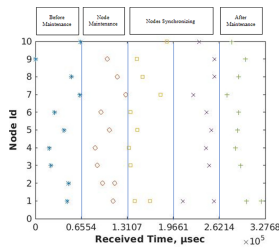


**Fig. 20.** Scheduling process of FAST for 10 nodes when a node is removed temporary

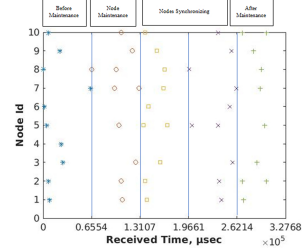


**Fig. 21.** Scheduling process of CSMA/CA for 10 nodes when a node is removed temporary

### 5.9 The Scheduling Effect During Node Addition

In this section, a new node will be added to the networks to evaluate the ability of the WBNs algorithms to maintain synchronicity. The new node introduced will cause the others nodes to hear the broadcast of the packet. The previous node and the next node to transmit will need to adjust its transmission time without affecting the order of node transmission.

The results from Fig. 22, Fig. 23 and Fig. 24 shows the synchronization process when a node added to the network with 5 nodes. From observations, the CSMA/CA has managed to maintained the transmission pattern while in FAST, only 30% of the nodes were in synchronicity after node added. However, in D-TDSP, it shown that the nodes were 100% synchronized after a node added. It can be seen from Fig. 22 that some of the node had delayed their transmission because of the synchronization error.

In the next set of results shown in Fig. 25, Fig. 26 and Fig. 27, the number of nodes in the networks is increased to 10 sensor nodes.

In this scenario, the D-TDSP and CSMA/CA show the nodes are transmitting in synchronizing pattern to the basestation compared to FAST. In D-TDSP, during the synchronization process, some of the nodes were seen transmitted twice in a period. This is because the synchronization convergence time was low. This will cause the nodes time to drift quickly and prompting the continuous resynchronization.

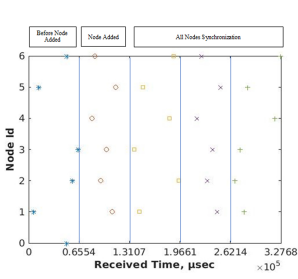


**Fig. 22.** Scheduling process of D-TDSP for 5 nodes when a node is added

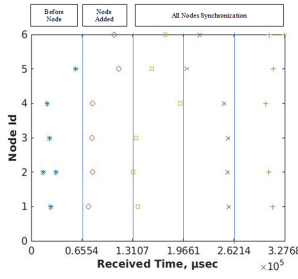


**Fig. 23.** Scheduling process of FAST for 5 nodes when a node is added

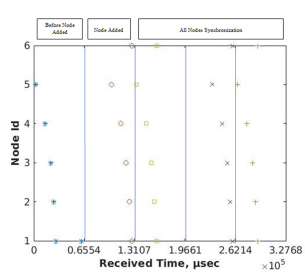


**Fig. 24.** Scheduling process of CSMA/CA for 5 nodes when a node is added

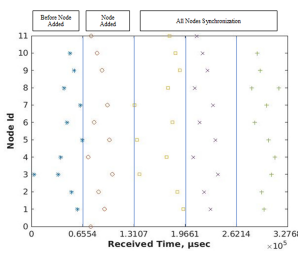


**Fig. 25.** Scheduling process of D-TDSP for 10 nodes when a node is added

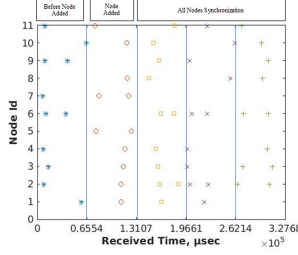


**Fig. 26.** Scheduling process of FAST for 10 nodes when a node is added

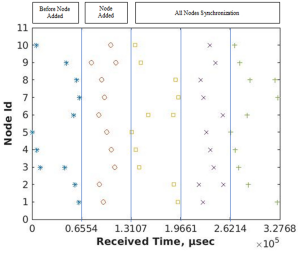


**Fig. 27.** Scheduling process of CSMA/CD for 10 nodes when a node is added

## 6 Discussion

From the results, it shown that D-TDSP has achieved the highest PDR compared to FAST and random CSMA/CA. As the number of sensor nodes increases, the D-TDSP can maintain the synchronicity of the data. It also shows that during node failure, D-TDSP can manage to transmit the packets in a synchronized period and patterns.

Similarly, when a node was added to the networks, D-TDSP is able to tolerate to temporary radio interference. Hence, any changes of the WBNS the D-TDSP will be able to recover and continue to broadcast the data to the basestation.

## 7 Conclusion

The results above shows that the proposed frog inspired algorithm, D-TDSP, has performed better than CSMA/CA and FAST. The results proved that when a node needed for maintenance, the D-TDSP managed to synchronize the packet data in a short time. Similarly, when there was addition of sensor nodes in the network, the algorithm can readjust its transmission interval. The D-TDSP is

able to synchronize the packet sequence and equally distributed the broadcast time of the sensor nodes and is tolerate to failure.

## References

1. Ashraf, D., Aboul Ella, H.: Wearable and implantable wireless sensor network solutions for healthcare monitoring. *Sensors* **11**(6), 5561–5595 (2011)
2. Campana, J., Gmelin, M., Schoechlin, J., Bolz, A.: Xml-based synchronization of mobile medical devices. *Biomed. Eng.* **47**, 857–9 (2002)
3. Dhruv, S., et al.: Wearable sensors for monitoring the physiological and biochemical profile of the athlete. *Biomed. Eng.* **47**, 857–9 (2002)
4. Ikkyu, A., Daichi, K., Yasuharu, H., Masayuki, M.: Mathematical modelling and application of frog choruses as an autonomous distributed communication system. *R. Soc. Open Sci.* **6**, 181117 (2019)
5. King, R.C., Villeneuve, E., White, R.J., Sherratt, R.S., Holderbaum, W., Harwin, W.S.: Application of data fusion techniques and technologies for wearable health monitoring. *Med. Eng. Phys.* **42**, 1–12 (2017)
6. Lim, T.H., Lau, H.K., Timmis, J., Bate, I.: Immune-inspired self healing in wireless sensor networks. In: Coello Coello, C.A., Greensmith, J., Krasnogor, N., Liò, P., Nicosia, G., Pavone, M. (eds.) *ICARIS 2012*. LNCS, vol. 7597, pp. 42–56. Springer, Heidelberg (2012). [https://doi.org/10.1007/978-3-642-33757-4\\_4](https://doi.org/10.1007/978-3-642-33757-4_4)
7. Maik, P., Steffen, M., Timo, T., Matthias, G., Reinhold, O.: Multi-modal signal acquisition using a synchronized wireless body sensor network in geriatric patients. *Biomed. Eng.* **61**(1), 57–68 (2016)
8. Monton, E., et al.: Body area network for wireless patient monitoring. *IET Commun.* **2**(2), 215–222 (2008)
9. Volmer, A., Orglmeister, R.: Wireless body sensor network for low-power motion-tolerant synchronized vital sign measurement. In: *Annual International Conference of the IEEE Engineering in Medicine and Biology Society*, pp. 3422–3425 (2008)
10. Wang, L., Lou, Z., Jiang, K., Shen, G.: Bio-multifunctional smart wearable sensors for medical devices. *Adv. Intell. Syst.* **1**(5), 1900040 (2019)
11. Werner-Allen, G., Tewari, G., Patel, A., Welsh, M., Nagpal, R.: Firefly-inspired sensor network synchronicity with realistic radio effects. In: *Proceedings of the 3rd International Conference on Embedded Networked Sensor Systems*, pp. 142–153 (2005)
12. Yildirim, K.S., Gurcan, O.: Efficient time synchronization in a wireless sensor network by adaptive value tracking. *IEEE Trans. Wirel. Commun.* **13**(7), 3650–3664 (2014)